NANO LETTERS

2007
Vol. 7, No. 12
3869−3874

Excitation Wavelength Dependence of Fluorescence Intermittency in CdSe/ZnS Core/Shell Quantum Dots

Kenneth L. Knappenberger, Jr., Daryl B. Wong, Yaroslav E. Romanyuk, and Stephen R. Leone*

Departments of Chemistry and Physics, University of California and Lawrence Berkeley National Laboratory, Berkeley, California 94720

Received June 21, 2007; Revised Manuscript Received September 21, 2007

ABSTRACT

Core/shell CdSe/ZnS quantum dot fluorescence-blinking statistics depend strongly on excitation wavelength. Excitation on the band gap (575 nm) results in inverse-power law "on" time distributions. However, distributions resulting from excitation above the band gap (525 nm) require a truncated power law and are 100 times less likely to display 10-s fluorescence. "Off" time statistics are insensitive to the excitation wavelength. The results may be explained by nonemissive trap states accessed with the higher-photon excitation energies.

Owing largely to the phenomenon of quantum confinement, semiconductor nanocrystals represent a promising class of inorganic materials with size- and shape-tunable properties. In particular, CdSe nanoparticles can be incorporated into devices with optical properties that are continuously tunable across the visible spectrum. Facile laboratory synthesis[1] of these nanoparticles with ever-increasing monodispersity has stimulated expectations ranging from quantum dot lasers,[2] hybrid photovoltaics,[3] and biological labels.[4] Parallel developments in measurement technologies have also prompted research into single-particle devices. For example, single-quantum dots can function as a one-photon source in an optical cavity, demonstrating potential for cryptography applications.[5] However, at the single-particle level quantum dots and nanorods exhibit complicated fluorescence intermittency or "blinking," exhibiting power law statistics over many decades in time.[6−11] These random interruptions of nanoparticle fluorescence emission can diminish the efficiency of devices based on single nanocrystals. Understanding the blinking mechanism is a necessary step for the ultimate implementation of quantum dots in electro-optic devices.

Fluorescence blinking is also ubiquitous in single-molecules. However, the blinking behavior of quantum dots is uniquely different from molecules. The probability distribution of fluorescent intervals of single-molecular dyes generally decays exponentially.[12] The on−off cycling kinetics of these molecules is accurately described by a three-state model known as a triplet bottleneck. Quantum dots on the other hand display a power law behavior over a wide range of times that is universal to all semiconductor nanomaterials studied to date,[13] which is suggestive of a common mechanism. In their original report,[6] Nirmal et al. attributed CdSe quantum dot blinking to an Auger-assisted ionization process, a low-probability event requiring a quadratic power density dependence of the excitation. This model was put into a theoretical framework by Efros and Rosen,[14] based on the supposition that a quantum dot with a net charge is nonemissive. The model suggests that upon excitation an electron or hole may become trapped, inducing a net charge in the particle. In the charged state, the quantum dot continues to absorb and a second electron−hole pair is formed. The primary dissipation pathway is a nonradiative mechanism that transfers energy to the excess charge carrier, thereby ejecting it from the nanoparticle. Photoluminescence would then recover as the particle regains neutrality. Evidence for net charge upon "photodarkening" has been reported.[15] However, this model predicts a single-exponential recovery rate for luminescence. Kuno et al.[7−9] reported fluorescence intermittency extending over eight decades of probability and six decades in time, described only by nonexponential power law statistics, fit to the form $P(t) = At^{-\alpha}$. It is now known that this behavior is typical of quantum dot-blinking statistics, and values of 3/2 are typically found for α. To account for the large dynamic range in both time and probability associated with quantum dot blinking, multiple trap states with a distribution of energies must be considered. Although much has been learned in the past decade about fluorescence intermittency in semiconductor nanocrystals, a unifying physical picture has not emerged.

* To whom correspondence should be addressed.

10.1021/nl0714740 CCC: $37.00 © 2007 American Chemical Society
Published on Web 11/10/2007

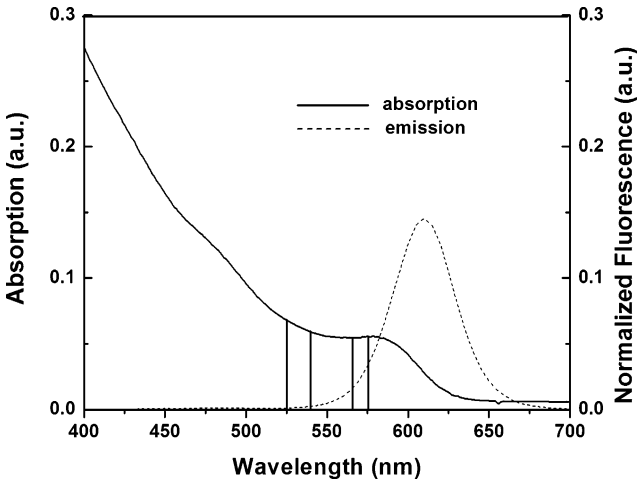

Figure 1. Bulk linear absorption and photoluminescence spectra of CdSe/ZnS quantum dots. The bulk absorption involves discrete excitonic features superimposed on a continuous background that increases to higher energies. The PL signal is Stokes-shifted from the first exciton at 580 nm by 30 nm and has a FWHM of 39 nm. The global PL is obtained from excitation with the 515 nm line of an Ar^+ laser. All measurements are performed in ambient conditions.

Here, we report on the excitation wavelength dependence of CdSe/ZnS core/shell quantum dot-blinking statistics. While previous work has shown that fluorescence-blinking statistics are sensitive to band gap separation,[10] this study provides the first in-depth investigation of the influence of excitation wavelength on the intermittency. The quantum dots are excited at several energies at and above the band gap (Figure 1) up to 85 nm or 330 meV above the peak of the photoluminescence emission; previous works employed only fixed-frequency excitation. The wavelength-dependent results reported here exhibit two types of blinking behavior: one that occurs when the sample is excited on or near the optical band gap and the other occurring when the excitation is well in excess of the band gap. The transition between these two types of behaviors appears to be step-like with excitation energy, which is suggestive of an energetic threshold. The creation of the electron−hole pair with energy in excess of the optical band gap results in less pronounced long-duration continuous emission events. The probability of observing continuous fluorescence that persists for 10 seconds decreases by as much as 2 orders of magnitude when the dots are excited well above the band gap. The findings suggest the overall performance of CdSe nanoparticle-based devices may strongly depend on the excitation wavelength.

The core/shell CdSe/ZnS quantum dots studied here are obtained from Evident Technologies (catalog number ED-C11-TOL-0600, lot number PJC011306). The bulk linear absorption and global photoluminescence (PL) spectra of the dots are shown in Figure 1. The PL spectrum is plotted normalized to the sample absorption for comparison. The linear absorption measurements are made on a dilute solution, while the PL measurement is obtained from a thin film of quantum dots spin-coated to a silica substrate. The peak of the first excitonic transition in absorption is centered at 580 nm, and absorption increases continuously to more energetic wavelengths. The peak of the PL is Stokes-shifted from the absorption by approximately 30 nm to 610 nm, and it has a full width at half-maximum (FWHM) of 39 nm. From the bulk absorption and PL measurements, a CdSe core size of 4.0 nm can be inferred. For single-nanoparticle studies, a dilute solution of the quantum dots is dissolved in toluene and spin-coated onto a 0.17 mm thick microscope coverslip (refractive index (n_D) = 1.515), resulting in a thin film of sparsely deposited particles. The coverslip is first cleaned by sonication in a Hellmanex II (Fluka) solution at 90 °C, followed by sonication in Millipore H_2O, and then several subsequent rinses to ensure removal of fluorescent impurities. The substrate is then passivated with *N*-(2-aminoethyl)-3aminopropyl-trimethoxysilane prior to quantum dot deposition. The deposition of single-particles is confirmed by atomic force microscopy (not shown).

The single-particle fluorescence trajectories are recorded using a home-built fluorescence microscope in an epi-illumination configuration. Two excitation sources are used: a continuous wave 543 nm laser and a high repetition rate wavelength-tunable femtosecond laser system. A Coherent Mira titanium sapphire oscillator produces femtosecond pulses that are amplified by a 200 kHz RegA regenerative amplifier, producing nominally 800 nm pulses with a temporal duration of 150 fs and pulse energies of 5 μJ. The laser output is split by a 70/30 beamsplitter to generate a 400 nm beam and a white-light continuum, which are then mixed in an optical parametric amplifier (Type I−BBO) to generate approximately 50 nJ of tunable output over a range of 500−700 nm. The intensities of both laser sources are attenuated with absorptive neutral density filters to provide average power densities at the sample ranging from 50 W/cm^2 to 10 kW/cm^2. This range of power densities allows for inclusion of both linear and nonlinear multiphoton excitation regimes. The lowest power density employed corresponds to an average per dot exciton density of ≈0.15. The excitation laser light is focused through the microscope slide onto the quantum dot sample on the reverse side. A diffraction-limited spot is obtained by an oil-immersion (n_D = 1.515) 1.3 NA objective (Nikon, PlanFluor 100), generating an approximately 200 nm spot size at the quantum dots. The sample is scanned through the focal volume with an *x*, *y*, *z* translation stage. The sample emission is collected through the same oil-immersion objective and directed through a series of dichroic and notch filters, isolating the band-edge emission prior to imaging individual quantum dots with a charge-coupled-device (CCD) detector. The signal is read out to a commercial video capture card and saved to a computer. The fluorescent point sources are temporally integrated to obtain fluorescence trajectories. The CCD detector has a readout time of 10 ms, providing the limit to the temporal resolution. The signal-to-noise ratio achieved for a single-dot trajectory with this apparatus using 10 ms binning is ≈4. Averages and standard deviations reported throughout the text are reported to $\pm 2\sigma$.

Fluorescence trajectories are obtained for single-quantum dots. A typical fluorescence trajectory resulting from continuous excitation at 543 nm with an excitation power density

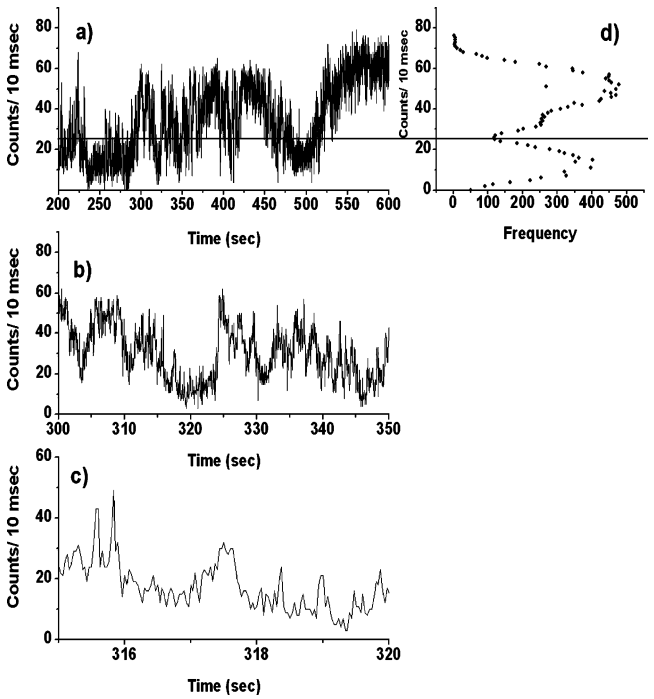

Figure 2. (a) Fluorescence trajectory for a single-CdSe/ZnS quantum dot. The same trajectory is reported on two additional different time scales in panels b and c. Random interruptions of fluorescence emission are observed on all time scales. The threshold employed to define fluorescent on and off intervals is also shown. (d) Plot summarizing the frequency of occurrences of the measured fluorescence intensities for panel a. A distinct gap between the signal and background levels, coinciding with the assigned threshold, is clearly evident.

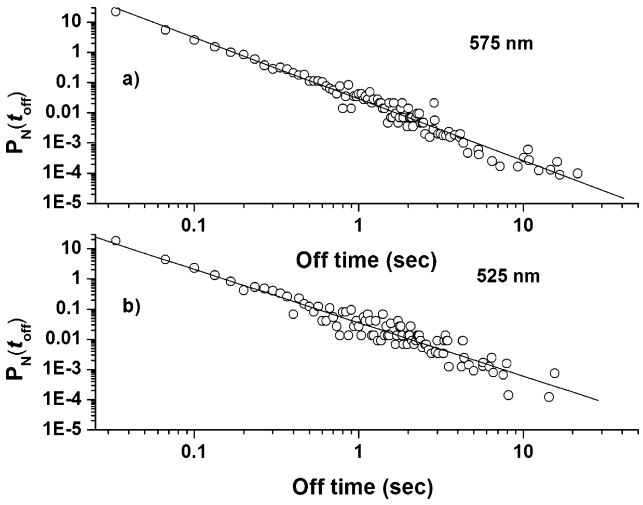

Figure 3. Wavelength-dependent normalized off behavior probabilities for individual quantum dots excited at 575 nm (a) and 525 nm (b). The probability densities are plotted on a log−log scale to extract the power law behavior. Statistically, the slopes ($\alpha_{off} \approx -1.6$) of the plots are insensitive to excitation wavelength. The slopes along with standard deviations obtained from more than 90 samples at each excitation wavelength are reported in Table 1.

of 80 W/cm^2 is shown in Figure 2a. The blinking phenomenon of single-quantum dots is evidenced by multiple interruptions of the particle's fluorescence emission at random intervals. Fluorescence trajectories are shown over three different time scales in Figures 2a−c, which exemplifes the random nature of the fluorescence blinking in CdSe nanocrystals, spanning a vast time range. The blinking statistics are analyzed by creating a probability distribution of "on" and "off" events of a given duration by first converting the fluorescence trajectory into a binary data set. The data are sorted into on and off categories by assigning a threshold, above which the quantum dot is considered on and below which it is considered off. The threshold level is assigned as twice the standard deviation above the average background counts. This procedure is similar to that used in reference 7. The validity of this method is demonstrated in Figure 2d, where the assigned threshold is plotted along with the intensity of count levels and their frequency of occurrence. The distinction between signal and noise levels is clearly made. For the analysis of on and off probabilities, it is sufficient to sort the data in this binary manner. However, the histogram of count levels shows that there is a distribution of signal levels for the on states, and the data clearly do not correspond to a single on intensity value or even a single Gaussian distribution of these levels. The complexity of the histogram suggests that a distribution of both emissive and nonemissive states is most likely responsible for the blinking mechanism, as suggested from time-resolved single-photon-counting measurements.[15]

The off probability distributions obtained from the CdSe/ZnS quantum dots when excited at 575 and 525 nm are shown plotted on a log−log scale in Figure 3, panels a and b, respectively. Excitation at the beginning of the optical band gap at 575 nm corresponds to an electronic transition to the first exciton band, whereas excitation at 525 nm promotes the electron to a higher continuum of electronic states. The off statistics are not sensitive to the exciting wavelengths or power densities over the ranges employed here. Corresponding to the random fluorescence fluctuations shown in Figure 2a, the normalized off probability distribution is clearly nonexponential and spans six decades of probability and five decades of time. These findings are consistent with previous reports[7−10] that support the hypothesis that a distribution of several nonemissive trap states with different energetic barriers is involved in the blinking process. The off probabilities measured here are fit to the well-known inverse power law with a slope α of -1.6 ± 0.2 for excitation at both 575 and 525 nm. A summary of the fit values along with the $\pm 2\sigma$ deviations is reported in Table 1. The lack of excitation wavelength dependence for the off statistics suggests that the recovery from an off to on configuration is not a photodriven process.

In contrast, the on data display significant sensitivity to excitation wavelength, as shown in Figure 4. The on statistics when excited at the beginning of the band gap (575 nm), Figure 4a, exhibit a good fit to a power law-normalized probability distribution with a slope α of -1.7 ± 0.1, and the on events extend as long as 100 s. Likewise, excitation at 565 nm ($\approx$160 meV above the band gap) also produces on probability distributions that are well described by a pure power law with an exponent α of -1.7 ± 0.1. This behavior is consistent with the reports of Kuno et al.[7−9] However,

Table 1. Summary of Fitting Results for On and Off Probabilities[a]

excitation wavelength	off analysis	on analysis	
	$-\alpha_{off}$	$-\alpha_{on}$	t_{on} (sec)
525 nm	1.6 ± 0.2	1.7 ± 0.2	4.0 ± 2.0
543 nm	1.5 ± 0.1	1.6 ± 0.2	6.0 ± 3.0
565 nm	1.6 ± 0.1	1.7 ± 0.1	NA
575 nm	1.6 ± 0.2	1.7 ± 0.1	NA

[a] Values reported are obtained from the average and standard deviation of several samples at each excitation wavelength, as shown in Figure 6. Standard deviations are reported to $\pm 2\sigma$.

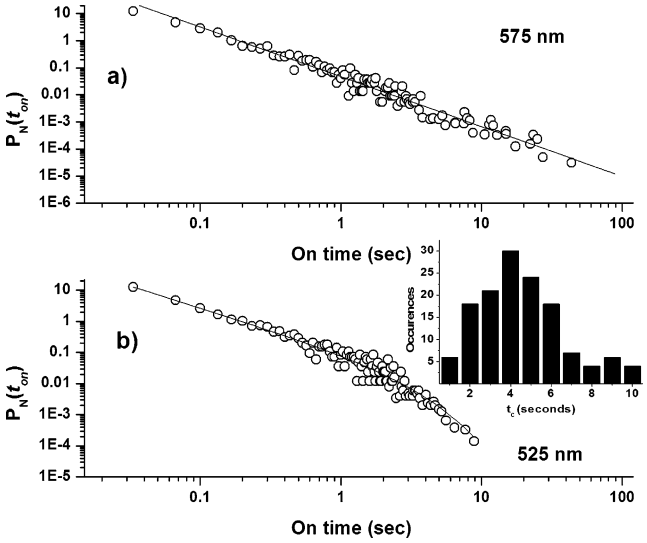

Figure 4. Wavelength-dependent normalized "on" behavior probabilities for individual quantum dots excited at 575 nm (a) and 525 nm (b), plotted on a log−log scale. The "on" statistics exhibit a significant dependence on the excitation wavelength. When excited on the band gap, as in panel a, the probability density exhibits an inverse power dependence at all observable time scales. However, upon excitation at more energetic wavelengths, panel b, a power law distribution is observed only for shorter duration events, while longer events fit an exponential decay. The inset of panel b includes a histogram representing the distribution of t_c values obtained from all of the >130 particles analyzed. The slopes and their standard deviations are reported for each excitation wavelength in Table 1.

when exciting with 525 nm light, which corresponds to approximately 330 meV above the band gap, the on statistics obey a power law for on events of short duration, but a distinct curvature is observed in the probability distribution plot due to much less pronounced on events of long duration. The probability distribution shown in Figure 4b can be fit to a truncated power law of form

$$P(t_{on}) = At_{on}^{-\alpha_{on}} e^{-t_{on}/t_c} \quad (1)$$

The truncation observed in the on time statistics, when excited above the band gap, results from decreased continuous fluorescence emission that persists beyond a few seconds. The transition between the two fluorescence emission behaviors is shown in Figure 5, where the probability of emission persisting for five distinct time intervals is plotted as a function of excitation wavelength. Figure 5 shows the

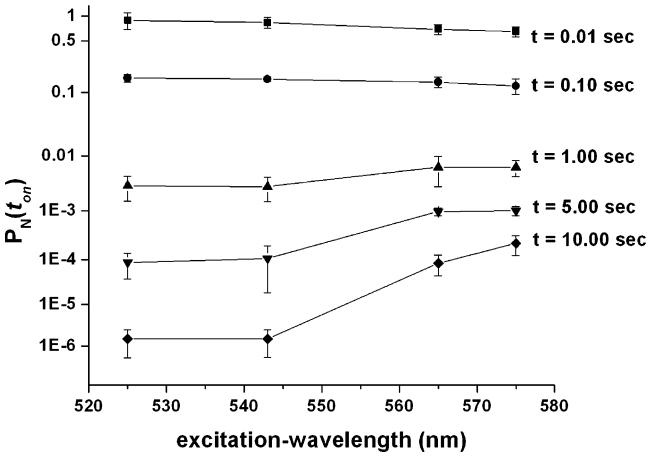

Figure 5. Excitation-wavelength dependence of fluorescence emission probabilities. The probabilities of observing continuous fluorescence emission for five distinct time durations (0.01, 0.1, 1.0, 5.0, and 10.0 s) are plotted as a function of each excitation wavelength. The plot shows a strong trend of fewer pronounced on events of long duration as the exciting photon energy is increased.

average and $\pm 2\sigma$ deviations in probability obtained from over 90 single-quantum dot fluorescence trajectories at each excitation wavelength. A decrease in probability is already observed for events lasting 1 s in going from 565 to 543 nm excitation wavelength, corresponding to 250 and 160 meV above the band gap. The decrease in probability becomes increasingly dramatic when longer duration events are considered (Figure 5). The probability of observing 10 s of continuous emission decreases by 2 orders of magnitude when going from 575 to 525 nm. Also, for the wavelengths where a deviation from power law statistics is observed (525 and 543 nm), the fitted values of t_c are the same within error, which is suggestive of an energetic threshold existing in the range between 160 and 250 meV above the band gap that leads to the behavior. The overall fit results for on statistics are reported in Table 1.

Curvature of the on probability distribution has been reported previously.[10,17] The behavior has been treated theoretically,[18] and the fitted parameters α_{on} and t_c reflect the slope of the power law component and the crossover time between intervals corresponding to power law and exponential behavior, respectively. Shimizu et al.[10] attributed the curvature to a "saturation" effect due to secondary mechanisms that limit the maximum on time of the quantum dot. In the previous studies,[10,17] CdSe particles were excited at a fixed-frequency above the band gap, employing excitation power densities spanning 175−700 W/cm^2. The deviation from a pure power law was found to be temperature-dependent, with "saturation" setting in at earlier times at higher temperatures.[10] Also, in the same study an excitation power dependence was observed at 10 K. Our investigation shows the curvature is dependent on the excitation wavelength and no significant dependence on power density is observed when exciting at room temperature. Our results are shown in Figure 6, where the fitted values and standard deviations of $-\alpha_{on}$ and t_{on} are reported in Figure 6, panels a and b, respectively, upon 543 nm excitation at various power

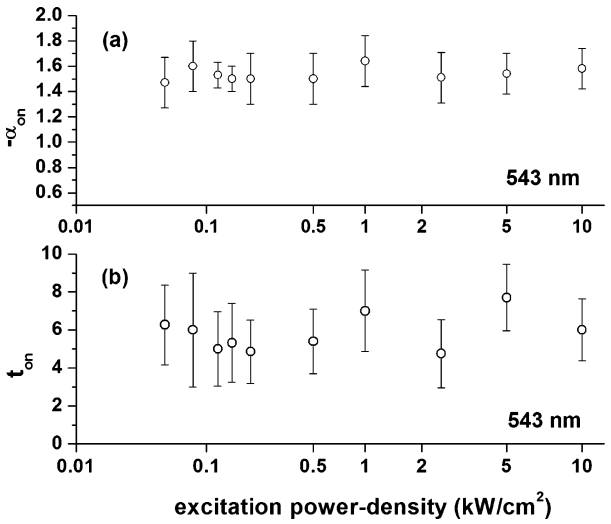

Figure 6. Summary of excitation power-dependent slopes ($-\alpha_{on}$) obtained from inverse-power law fit to the on probability distributions and t_{on} values for all samples investigated at an excitation wavelength of 543 nm. Results for the slopes of on statistics are shown in panel a. Likewise t_{on} values vs power density are shown in panel b. Statistically, the slopes and t_{on} values are not influenced by the excitation power density. Averages and standard deviations reported throughout the text are determined to $\pm 2\sigma$.

densities. The values obtained for both the α_{on} and t_{on} are not statistically influenced by the excitation power density. The influence of an excitation power dependence at 10 K, but not at room temperature, is most likely indicative of a phonon-assisted process that is involved in the blinking, and this is consistent with the wavelength-dependent results here.

In the present study, the value of $-\alpha_{on}$ is typically $(1.5-1.7) \pm 0.2$ and is independent of excitation wavelength, as reported in Table 1. As is typical of colloidally synthesized nanoparticles, the sample consists of a distribution of particle sizes. As such, complete statistics are only obtained by investigating a large, representative sample. The distribution of t_{on} values obtained for over 130 individual dots is shown in the inset of Figure 4b, where one can clearly see the truncation at long times. The value obtained for t_{on} is 4.0 ± 2.0 s at 525 nm. A very similar on time probability distribution is obtained when exciting approximately 250 meV above the band gap at 543 nm (cw laser), regardless of excitation power density. The value obtained for t_{on} at 543 nm is 6 ± 3. The linearities obtained in the log−log plots for the off distributions and the on distributions recorded near the band gap clearly indicate that the curvature in the on distributions measured at more energetic excitation wavelengths is not the result of an artifact. In fact, the values determined for t_{on} are approximately the same as those previously reported for nanocrystals, where blinking was studied only with excitation well above the band gap.[11] Attempts to fit the probability distributions obtained for excitation at both 525 and 543 nm to a pure power law and a pure exponential function provide unsatisfactory results. Also, to confirm that the wavelength-dependent results are not a result of the nanoparticle sample batch, a second set of CdSe quantum dots obtained from an independent source was measured. The wavelength dependence was reproduced, suggesting a mechanism intrinsic to the CdSe nanocrystals.

Although the current data present a first in-depth look at excitation wavelength-dependent-blinking statistics in quantum dots, the findings are consistent with previous results at selected wavelengths, also noted above, and with PL and related experiments. The lack of long-duration continuous fluorescence emission events observed here, as well as an increase in cycling between on and off states, can be correlated with the reported decrease in the fluorescence quantum yield with increasing excitation-photon energy. In fact, bulk photoluminescence excitation measurements show that fluorescence quantum yields decrease by as much as 50% for CdSe quantum dots in an abrupt, steplike manner when excited at ≈300 meV(60 nm) above the band gap.[19] The decrease of the measured quantum yield reaches a plateau beyond this energetic region. This threshold is similar to our on time distributions for single-quantum dot blinking. Differences in the values of energetic thresholds may occur from sample to sample as a result of differences in sample size, due to dissimilar spacing of quantized levels. This quantum yield behavior was reproduced in InP quantum dots.[20,21] In InP quantum dots, decreased PL efficiency was observed when exciting just beyond the first exciton band. The exact mechanism is unknown, but the result was attributed to either ionization of a valence electron to a continuum of electronic states in the conduction band or to the filling of nonemissive surface traps. The former mechanism results from removal of an electron preferentially instead of radiative decay. Spectral diffusion in single-CdSe nanocrystals is also shown to be excitation wavelength-dependent with more energetic pump photons exhibiting a greater degree of spectral broadening of emission.[22] The mechanism is believed to arise from surface charging, inducing a Stark-shift of the band gap energy. A strong temperature dependence was also observed with the broadening mechanism becoming pronounced above 40 K, suggesting a thermally activated charging mechanism. Finally, quantum dot size has been reported to influence the on probability distribution of single quantum dots.[10] Although the effect was small, larger dots were found to deviate from power law statistics at earlier times than smaller ones when excited with a fixed wavelength. This size effect also corresponds to an energetic effect, as the larger dot has a smaller band gap separation. Although the study reported in reference 10 does not allow a direct comparison due to differences in surface/volume ratio with changing particle size, their experimental observations are consistent with the findings here.

Ultrafast ensemble measurements of CdSe exciton decay pathways have also been measured at room temperature,[23,24] which are relevant to our studies. From this work, it is known that upon vertical excitation the electron preferentially relaxes nonradiatively to the bottom of the conduction band as it dissipates excess energy to discrete phonon modes. Subsequently, radiative recombination may occur, or the electron may fill surface traps via phonon-assisted mechanisms. Phonon modes were also suggested to play a critical role in

spectral diffusion.[22] The wavelength dependence observed in our blinking studies, taken together with existing literature, suggests that an energetic threshold on the order of 200 meV exists, which leads to a population of nonemissive states that play a significant role in the blinking process. These traps may be populated directly as the electron is relaxing to the bottom of the conduction band or alternatively may be accessed via phonon-assisted mechanisms. Such an explanation is also consistent with the temperature dependence observed in previous blinking studies.[10]

It is important to note that the present study alone does not preclude the possibility that tunneling events or nonlinear processes contribute to the blinking mechanism, as it is a complex process that is only partly understood. But the results do demonstrate the importance of intermediate steps in the blinking process and also show that blinking is observed clearly in both linear and nonlinear excitation regimes. Currently, we are investigating blinking statistics in zero-dimensional- and one dimensional- confined CdSe nanoparticles in a variety of environmental conditions. We are also investigating temperature- and wavelength-dependent global photoluminescence to obtain a more complete picture of the mechanisms leading to quantum dot fluorescence intermittency.

In conclusion, we have presented excitation wavelength-dependent results for the blinking statistics of single-CdSe/ZnS quantum dots. Whereas the off statistics are not influenced by excitation wavelength or power density, the on statistics are found to be sensitive to the exciting wavelength. Qualitatively, the quantum dots cycle from on to off configurations more frequently when excitation promotes the electron well above the band gap than when the excitation frequency is near resonance with the first exciton transition. The on probability distributions that result from these two distinct excitation regimes on the badgap resonance and with energy in excess of the band gap can be fit quantitatively to two different models: a power law and a truncated power law, respectively. The truncated power law reflects a limitation to the duration of on-events. The data indicate a wavelength-dependent-blinking mechanism that limits the continuous fluorescence emission efficiency of CdSe nanoparticles resulting from multiple nonemissive trap states spanning a distribution of energies. A possible explanation is that higher photon energies access trap states more readily than when the minimum energy is used to create the charge carriers. The findings suggest the performance efficiency of quantum dot-based devices could be strongly dependent on the exciting wavelength.

Acknowledgment. The authors gratefully acknowledge financial support by the Director, Office of Basic Energy Sciences, Chemical Sciences, Geosciences, and Biosciences Division, U.S. Department of Energy under Contract No. DE-AC02-05CH11231.

References

(1) Murray, C. B.; Norris, D. J.; Bawendi, M. G. *J. Am. Chem. Soc.* **1993**, *115*, 8706.
(2) Klimov, V. I.; Mikhaelovsky, A. A.; Xu, S.; Mlko, A.; Hollingsworth, J. A. *Science* **2000**, *290*, 314.
(3) Huynh, W. U.; Dittmer, J. J; Alivisatos, A. P. *Science* **2002**, *290*, 2425.
(4) Bruchez, M. P.; Moronne, M.; Gin, P.; Weiss, S.; Alivisatos, A. P. *Science* **1998**, *281*, 2013.
(5) Santori, C.; Gotzinger, S.; Yamamoto, Y.; Kako, S.; Hoshino, K.; Arakawa, Y. *Appl. Phys. Lett.* **2005**, *87*, 051916.
(6) Nirmal, M.; Dabbousi, B. O.; Bawendi, M. G.; Macklin, J. J.; Trautman, J. K.; Harris, T. D.; Brus, L. E. *Nature* **1996**, *383*, 802.
(7) Kuno, M.; Fromm, D. P.; Hamann, H. F.; Gallagher, A.; Nesbitt, D. J. *J. Chem. Phys.* **2000**, *112*, 3117.
(8) Kuno, M.; Fromm, D. P.; Hamann, H. F.; Gallagher, A,; Nesbitt, D. J. *J. Chem. Phys.* **2001**, *115*, 1028.
(9) Kuno, M.; Fromm, D. P.; Johnson, S. T.; Gallagher, A.; Nesbitt, D. J. *Phys. Rev. B* **2003**, *67*, 125304.
(10) Shimizu, K. T.; Neuhauser, R. G.; Leatherdale, C. A.; Empedocles, S. A.; Woo, W. K.; Bawendi, M. G. *Phys. Rev. B* **2001**, *63*, 205316.
(11) Wang, S.; Querner, C.; Emmons, T.; Drndic, M.; Crouch, C. H. *J. Phys. Chem. B* **2006**, *110*, 23221.
(12) Yip, W.-T.; Dehong, H.; Yu, J.; Vanden Bout, D. A.; Barbara, P. F. *J Phys. Chem. A* **1998**, *102*, 7564.
(13) Kuno, M.; Fromm, D. P.; Gallagher, A.; Nesbitt, D. J.; Micic, O. I.; Nozik, A. J. *Nano Lett.* **2001**, *1*, 557.
(14) Efros, A. L.; Rosen, M. *Phys. Rev. Lett.* **1997**, *78*, 1110.
(15) Krauss, T. D.; Brus, L. E. *Phys. Rev. Lett.* **1999**, *83*, 4840.
(16) Zhang, K.; Chang, H.; Fu, A.; Alivisatos, A. P.; Yang, H. *Nano Lett.* **2006**, *6*, 843.
(17) Heyes, C. D.; Kobitski, A. Y.; Breus, V. V.; Nienhaus, G. U. *Phys. Rev. B* **2007**, *75*, 125431.
(18) Tang, J.; Marcus, R. *J. Chem. Phys.* **2005**, *123*, 054704.
(19) Hoheisel, W.; Colvin, V. L.; Johnson, C. S.; Alivisatos, A. P. *J. Chem. Phys.* **1994**, *101*, 8455.
(20) Rumbles, G.; Selmarten, D. C.; Ellingson, R. J.; Blackburn, J. L.; Yu, P.; Smith, B. B.; Micic, O, I.; Nozik, A. J. *J. Photochem. Photobiol. A* **2001**, *142*, 187.
(21) Ellingson, R. J.; Blackburn, J. L.; Yu, P.; Rumbles, G.; Micic, O. I.; Nozik, A. J. *J. Phys. Chem. B* **2002**, *106*, 7758.
(22) Empedocles, S. A.; Bawendi, M. G. *J. Phys. Chem. B* **1999**, *103*, 1826.
(23) Klimov, V. I.; Bawendi, M. G. *MRS Bulletin* **2001**, 998.
(24) Schill, A. W.; Gaddis, C. S.; Qian, W.; El-Sayed, M. A.; Cai, Y.; Milan, V. T.; Sandhage, K. *Nano Lett.* **2006**, *6*, 1940.

NL0714740